Dark solitons manipulation using optical event horizon

ZHIXIANG DENG,[1] JUN LIU,[2,3,*] XIANWEI HUANG,[4] CHUJUN ZHAO,[5] AND XINLIN WANG[1,6]

[1]School of Electrical Engineering, University of South China, Hengyang 421001, China
[2]International Collaborative Laboratory of 2D Materials for Optoelectronics Science and Technology, Key Laboratory of Optoelectronic Devices and Systems of Ministry of Education and Guangdong Province, College of Optoelectronic Engineering, Shenzhen University, Shenzhen 518060, China
[3]Aston Institute of Photonic Technologies, School of Engineering and Applied Science, Aston University, Birmingham B4 7ET, UK
[4]College of Computer Science and Electronic Engineering, Hunan University, Changsha 410082, China
[5]Laboratory for Micro-/Nano- Optoelectronic Devices of Ministry of Education, IFSA Collaborative Innovation Center, School of Physics and Electronics, Hunan University, Changsha 410082, China
[6]wxl_ly000@aliyun.com
[*]j.liu26@aston.ac.uk

Abstract: We demonstrate that the optical event horizon can provide an effective technique to actively control the propagation properties of a dark soliton with another weak probe wave. Careful power adjustment of the probe wave enables the black soliton converted into a gray one with varying grayness through the nonlinear interaction, corresponding to a nearly adiabatic variation of the soliton's speed. The sign of the phase angle for the newly formed gray soliton at optical event horizon is significantly dependent on the frequency of the launched probe wave. Linear-stability analysis of dark solitons under the perturbation of a weak probe wave is performed to clarify the intrinsic mechanism of the nonlinear interaction. The probe wave manipulated collisional dynamics between both dark solitons are investigated as an analogue of the combined white-hole and black-hole horizons which provides some insights into exploring the transition between integrable and non-integrable systems.

References and links

1. A. Demircan, Sh. Amiranashvili, and G. Steinmeyer, "Controlling light by light with an optical event horizon," Phys. Rev. Lett. **106**(16), 163901 (2011).
2. P. Kanakis and T. Kamalakis, "Enabling transistor-like action in photonic crystal waveguides using optical event horizons," Opt. Lett. **41**(7), 1372–1375 (2016).
3. D. V. Skryabin and A. V. Gorbach, "Colloquium: Looking at a soliton through the prism of optical supercontinuum," Rev. Mod. Phys. **82**(2), 1287–1299 (2010).
4. L. Tartara, "Soliton control by a weak dispersive pulse," J. Opt. Soc. Am. B **32**(3), 395–399 (2015).
5. S. Pickartz, U. Bandelow, and S. Amiranashvili, "Adiabatic theory of solitons fed by dispersive waves," Phys. Rev. A **94**(3), 033811 (2016).
6. T. G. Philbin, C. Kuklewicz, S. Robertson, S. Hill, F. König, and U. Leonhardt, "Fiber-optical analog of the event horizon," Science **319**(5868), 1367–1370 (2008).
7. S. F. Wang, A. Mussot, M. Conforti, A. Bendahmane, X. L. Zeng, and A. Kudlinski, "Optical event horizons from the collision of a soliton and its own dispersive wave," Phys. Rev. A **92**(2), 023837 (2015).
8. A. V. Yulin, R. Driben, B. A. Malomed, and D. V. Skryabin, "Soliton interaction mediated by cascaded four wave mixing with dispersive waves," Opt. Express **21**(12), 14481–14486 (2013).
9. M. A. Gaafar, A. Y. Petrov, and M. Eich, "Free carrier front induced indirect photonic transitions: A new paradigm for frequency manipulation on chip," ACS Photonics **4**(11), 2751–2758 (2017).
10. K. E. Webb, M. Erkintalo, Y. Xu, N. G. Broderick, J. M. Dudley, G. Genty, and S. G. Murdoch, "Nonlinear optics of fibre event horizons," Nat. Commun. **5**(1), 4969 (2014).
11. A. Efimov, A. V. Yulin, D. V. Skryabin, J. C. Knight, N. Joly, F. G. Omenetto, A. J. Taylor, and P. Russell, "Interaction of an optical soliton with a dispersive wave," Phys. Rev. Lett. **95**(21), 213902 (2005).

12. I. Oreshnikov, R. Driben, and A. V. Yulin, "Interaction of high-order solitons with external dispersive waves," Opt. Lett. **40**(23), 5554–5557 (2015).
13. A. Choudhary and F. König, "Efficient frequency shifting of dispersive waves at solitons," Opt. Express **20**(5), 5538–5546 (2012).
14. A. Bendahmane, A. Mussot, M. Conforti, and A. Kudlinski, "Observation of the stepwise blue shift of a dispersive wave preceding its trapping by a soliton," Opt. Express **23**(13), 16595–16601 (2015).
15. I. Oreshnikov, R. Driben, and A. V. Yulin, "Weak and strong interactions between dark solitons and dispersive waves," Opt. Lett. **40**(21), 4871–4874 (2015).
16. Z. X. Deng, X. H. Shi, C. Tan, and X. Q. Fu, "Reversible conversion between optical frequencies of probe and idler waves in regime of optical event horizon," J. Opt. Soc. Am. B **33**(5), 857–863 (2016).
17. A. Demircan, S. Amiranashvili, C. Brée, and G. Steinmeyer, "Compressible octave spanning supercontinuum generation by two-pulse collisions," Phys. Rev. Lett. **110**(23), 233901 (2013).
18. X. Liu, B. Zhou, H. Guo, and M. Bache, "Mid-IR femtosecond frequency conversion by soliton-probe collision in phase-mismatched quadratic nonlinear crystals," Opt. Lett. **40**(16), 3798–3801 (2015).
19. Z. Deng, X. Fu, J. Liu, C. Zhao, and S. Wen, "Trapping and controlling the dispersive wave within a solitonic well," Opt. Express **24**(10), 10302–10312 (2016).
20. S. F. Wang, A. Mussot, M. Conforti, X. L. Zeng, and A. Kudlinski, "Bouncing of a dispersive wave in a solitonic cage," Opt. Lett. **40**(14), 3320–3323 (2015).
21. Z. X. Deng, J. Liu, X. W. Huang, C. J. Zhao, and X. L. Wang, "Active control of adiabatic soliton fission by external dispersive wave at optical event horizon," Opt. Express **25**(2–3), 28556–28566 (2017).
22. Y. S. Kivshar and B. Luther-Davies, "Dark optical solitons: physics and applications," Phys. Rep. **298**(2/3), 81–197 (1998).
23. A. Hasegawa and F. Tappert, "Transmission of stationary nonlinear optical pulses in dispersive dielectric fibers. II. Normal dispersion," Appl. Phys. Lett. **23**(4), 171–172 (1973).
24. P. Emplit, J. P. Hamaide, F. Reynaud, C. Froehly, and A. Barthelemy, "Picosecond steps and dark pulses through nonlinear single mode fibers," Opt. Commun. **62**(6), 374–379 (1987).
25. D. J. Frantzeskakis, "Dark solitons in atomic Bose-Einstein condensates: From theory to experiments," J. Phys. A Math. Theor. **43**(21), 213001 (2010).
26. A. Muryshev, G. V. Shlyapnikov, W. Ertmer, K. Sengstock, and M. Lewenstein, "Dynamics of dark solitons in elongated Bose-Einstein condensates," Phys. Rev. Lett. **89**(11), 110401 (2002).
27. V. V. Afanasjev, C. R. Menyuk, and Y. S. Kivshar, "Effect of third-order dispersion on dark solitons," Opt. Lett. **21**(24), 1975–1977 (1996).
28. A. Mahalingam and K. Porsezian, "Propagation of dark solitons with higher-order effects in optical fibers," Phys. Rev. E **64**(4), 046608 (2001).
29. C. Milián, D. V. Skryabin, and A. Ferrando, "Continuum generation by dark solitons," Opt. Lett. **34**(14), 2096–2098 (2009).
30. T. Marest, C. Mas Arabí, M. Conforti, A. Mussot, C. Milián, D. V. Skryabin, and A. Kudlinski, "Emission of dispersive waves from a train of dark solitons in optical fibers," Opt. Lett. **41**(11), 2454–2457 (2016).
31. T. Marest, C. M. Arabí, M. Conforti, A. Mussot, C. Milián, D. V. Skryabin, and A. Kudlinski, "Grayness-dependent emission of dispersive waves from dark solitons in optical fibers," Opt. Lett. **43**(7), 1511–1514 (2018).
32. C. Milián, T. Marest, A. Kudlinski, and D. V. Skryabin, "Spectral wings of the fiber supercontinuum and the dark-bright soliton interaction," Opt. Express **25**(9), 10494–10499 (2017).
33. S. Robertson and U. Leonhardt, "Frequency shifting at fiber-optical event horizons: the effect of Raman deceleration," Phys. Rev. A **81**(6), 063835 (2010).
34. S. Batz and U. Peschel, "Diametrically driven self-accelerating pulses in a photonic crystal fiber," Phys. Rev. Lett. **110**(19), 193901 (2013).
35. M. Sciacca, C. F. Barenghi, and N. G. Parker, "Matter-wave dark solitons in boxlike traps," Phys. Rev. A **95**(1), 013628 (2017).
36. C. M. Arabí, F. Bessin, A. Kudlinski, A. Mussot, D. Skryabin, and M. Conforti, "Efficiency of four-wave mixing between orthogonally polarized linear waves and solitons in a birefringent fiber," Phys. Rev. A **94**(6), 063847 (2016).
37. W. M. Cao and B. Y. Guo, "Fourier collocation method for solving nonlinear Klein-Gordon equation," J. Comput. Phys. **108**(2), 296–305 (1993).
38. D. E. Pelinovsky and P. G. Kevrekidis, "Dark solitons in external potentials," Z. Angew. Math. Phys. **59**(4), 559–599 (2008).
39. J. H. Nguyen, P. Dyke, D. Luo, B. A. Malomed, and R. G. Hulet, "Collisions of matter-wave solitons," Nat. Phys. **10**(12), 918 (2014).
40. R. N. Thurston and A. M. Weiner, "Collisions of dark solitons in optical fibers," J. Opt. Soc. Am. B **8**(2), 471–477 (1991).
41. R. I. Woodward and E. J. R. Kelleher, "Dark solitons in laser radiation build-up dynamics," Phys Rev E **93**(3), 032221 (2016).

1. Introduction

Light-by-light controlling, as we know, is considered the cornerstone of optical signal processing application such as future optical transistor-like devices [1,2]. One of the effective approaches to realize this is by applying the well-known cross-phase-modulation (XPM) effect arising from Kerr-nonlinear media [3–5]. With suitable conditions one may observe strong interaction between an intense optical soliton pulse and a weak probe pulse that results in an optical analogue of the gravitational phenomenon known as event horizons [6]. This analogue occurs in typical occasions where the weaker probe wave cannot penetrate through the optical soliton pulse during their collision process. The underlying physics was described in the time domain in terms of a soliton-induced refractive index barrier (Kerr effect) that changes the velocity of the probe wave [7–9]. The fundamental mechanism can also be interpreted in the frequency-domain [10] since the velocity variation of the probe wave is directly resulting from the generation of new spectral components [11–15]. It is worth mentioning that the frequency conversion process is reversible [16]. The optical event horizons created by nonlinear collision between pulses in an optical fiber have attracted considerable attention in recent years [17–21]. Researchers found that the essential mechanism for new frequency generation at optical event horizon can be applied as a potentially effective method for highly coherent supercontinuum generation without soliton fissions and modulation instability [17, 18]. Moreover, it has been numerically [8, 12, 19] and experimentally [20] shown that a weak DW can be produced and trapped within a solitonic cavity formed by two solitons at optical event horizon. To date, the reported results involving optical event horizon focus mainly on the active control of fundamental [1–5] or higher-order bright solitons [12, 21] by a weak probe wave and the scattering of a weak probe wave from solitons [7, 15–18, 20]. However, to the best of our knowledge, the tunable propagation properties of dark solitons, the basic physics behind which is quite fundamental and different to that involving the bright solitons, have not been systematically explored with optical event horizon so far.

Optical dark solitons, existing only in the regime of normal group-velocity dispersion (GVD), exhibit a local notch over their uniform intensity background with a phase slip across it, and travel with constant velocity and unchangeable profile [22]. Dark solitons were predicted [23] and experimentally [24] observed as early as several decades ago. Since then they had gained considerable attention, and have been studied in various branches of physics [22, 25, 26], especially in the field of nonlinear optics [27–32]. The dark soliton dynamics in optical fibers under the perturbation of higher-order dispersive and nonlinear effects have been investigated numerically [27–29] and experimentally [30, 31] where emission of DWs can be observed with their frequency and amplitude largely dependent on the soliton grayness. Recently, researchers reported that the short and long wavelength wings of the fiber supercontinuum spectrum can be shaped by the collision and interaction of the dark and bright solitons [32]. This dark pulse collision phenomenon continues to be a topic of contemporary research.

Here, we show numerically the nonlinear interaction between dark solitons and weak probe waves at optical event horizon and analyze the mechanism behind through the linear-stability analysis of dark solitons under the probe wave perturbation, which can provide innovative perspectives into the light-by-light control. We demonstrate that the dynamics of optical dark solitons can be manipulated by a weak probe wave carefully adjusted at the input in terms of peak power and frequency detuning. Besides, it is shown that the weak probe wave can induce a dissipative effect upon the dark soliton in terms of amplitude decay and oscillated tail generation, and the "catastrophic collapse" of the dark soliton is associated with an exponential growth of a perturbation induced by cross-phase-modulation. We also explore the possibility of manipulating of the nonlinear collision between both dark solitons by the probe waves with varied peak powers.

2. Propagation model

To gain physical insights into the optical event horizon dynamics, we employ the symmetric Fourier split-step method to solve the non-integrable nonlinear Schrödinger equation (NLSE) governing the pulse propagation in dispersive nonlinear media, as following [8,10]:

$$\frac{\partial A(z,T)}{\partial z} = iD(i\partial_T)A(z,T) + i\gamma \mid A(z,T) \mid^2 A(z,T). \tag{1}$$

Here, $D(i\partial_T) = \sum_{n\geq 2}\frac{\beta_n}{n!}(i\partial_T)^2$ is the dispersion operator which takes into account the fiber dispersion profile up to the third order ($n = 3$), $\beta_2 = 3.3708$ ps^2/km, $\beta_3 = 4.2977 \times 10^{-2}$ ps^3/km and $\gamma = 2.5$ W^{-1}/km is the nonlinear coefficient denoting the strength of nonlinear interactions. The nonlinear dynamics involved in light-by-light controlling here is mainly determined by the third-order nonlinear optical Kerr effect. It is worth noting that for the sake of brevity we neglect the stimulated Raman scattering effect. Although the Raman effect clearly affects dark pulse propagation, it is trivial for the main concept of a optical event horizon with light-by-light control [33]. Apart from the dominant terms of Kerr and normal GVD that are required to form dark solitons, we also include the third-order dispersion term in the full model in order to obtain the regime of optical event horizon. It has been found that the higher-order dispersion with $n>3$ and self-steepening (SS) term do not play any significant role [5, 33].
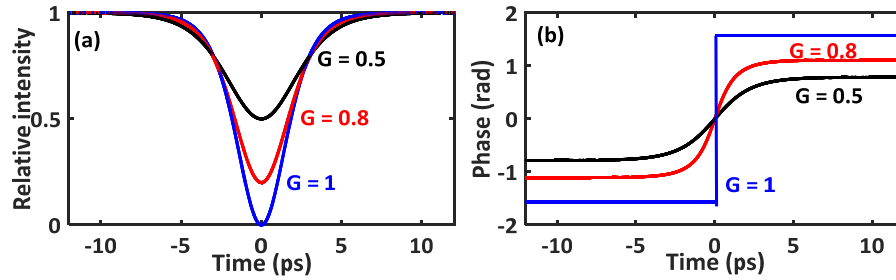

Fig. 1. Definition of a dark soliton, showing the relative intensity (a) and phase (b) of a black soliton ($G = 1$) and two gray solitons ($G = 0.8$ and 0.5). G denotes the soliton grayness. The remaining parameters are fixed to $T_0 = 0, A_0 = 1$.

The input light consists of two pulses launched with different frequencies namely the dark pulse and the probe wave. The overall electric field of the input light is determined as following:

$$A(T) = A_{ds}(T) + A_p(T), \tag{2}$$

where the initial form of the probe wave is given by a Gaussian pulse with a relative frequency detuning of $\Delta\omega$:

$$A_p(T) = \sqrt{P_p} \exp\left[-\left(\frac{T-t_1}{T_1}\right)^2\right]\exp(-i\Delta\omega T) \tag{3}$$

Here, P_p represents the peak power of the probe wave, $t_1 = 3.5$ ps and $T_1 = 850$ fs denote the temporal delay and width of the probe wave, respectively. The electric field of the dark soliton is given by [22]

$$A_{ds}(T) = A_0 \left\{ \cos\phi \tan h[A_0 \cos\phi(T - T_0)] + i\sin\phi \right\} \tag{4}$$

where A_0 represents the background amplitude of the dark soliton and ϕ is the soliton phase angle ($|\phi| \leq \pi/2$) describing the phase shift of the dark soliton, and its soliton grayness ($\cos\phi$) as well as the velocity ($\sin\phi$). The relative intensity and phase of the dark-soliton are typically plotted in Fig. 1. The blue curves illustrated in Fig. 1 is given under the limiting case of $\phi = 0$ where Eq. (4) reduces to

$$A_{ds}(T) = A_0 \tan h[A_0(T - T_0)], \tag{5}$$

where the intensity goes to zero at the center T_0 of the pulse, and this has been referred as the stationary black soliton. It can be seen that the black solitons are odd pulses characteristic of a π phase jump at the center part where the intensity is zero. The dark pulses with $\phi \neq 0$ that are known as gray solitons, have a similar but smaller and slower phase shift at their core where the intensity is minimized, as shown in Fig. 1(b). The time-dependent phase-shift represents an effective frequency shift, resulting in a slightly different propagation velocity from that at the carrier frequency used to define our retarded reference frame.
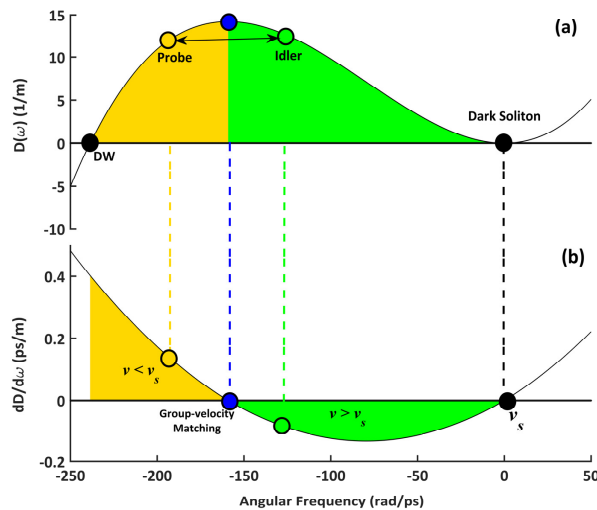

Fig. 2. Wavenumber and corresponding retarded-frame group-velocity as a function of angular frequency, illustrating how phase-matched probe-idler pairs experience group-velocities with opposite signs relative to soliton. In the soliton-probe wave interaction process, both the frequencies of the probe and idler waves are swapped. In the retarded reference frame, optical waves with frequencies falling in the green (orange)-shaded area propagate more slowly (quickly) than the dark soliton. DW: dispersive wave generated by the phase-matched resonant excitation.

3. Results and discussions

3.1 Propagation dynamics of dark solitons manipulated with a probe wave

The nonlinear collision dynamics between a soliton pulse and a probe wave can create a group-velocity-led optical event horizon for specific probe frequencies, which can provide the potential technique to manipulate the dark soliton by the weak probe wave. The main prerequisite for the group-velocity-led optical event horizon is to establish an effective refractive index barrier and make the group velocities reasonably close for both the soliton and the probe wave. In Fig. 2, we show a typical cubic dispersion relation characteristic of a

step-index single-mode fiber in the following numerical simulations, as well as the corresponding retarded-frame group-velocity. Here, $D(\omega)=\beta(\omega)-\beta(\omega_s)-\beta_1\times(\omega-\omega_s)$, where $\beta(\omega)$ is the fiber propagation constant, and $\beta_1=\partial_\omega\beta(\omega_s)$ is the group velocity at the soliton frequency ω_s; v_s is the group velocity of the dark soliton (highlighted as a horizontal line). The green (yellow)-shaded area in the frequency region represents the fiber-optical analogue of black (white)-hole horizon in which the probe appears to be visibly reflected on the trailing (leading) edge of soliton, with the resulting frequency up- (down-) converted. The frequency that is group velocity matched to the dark soliton represents the transition point between white- and black-hole horizons.
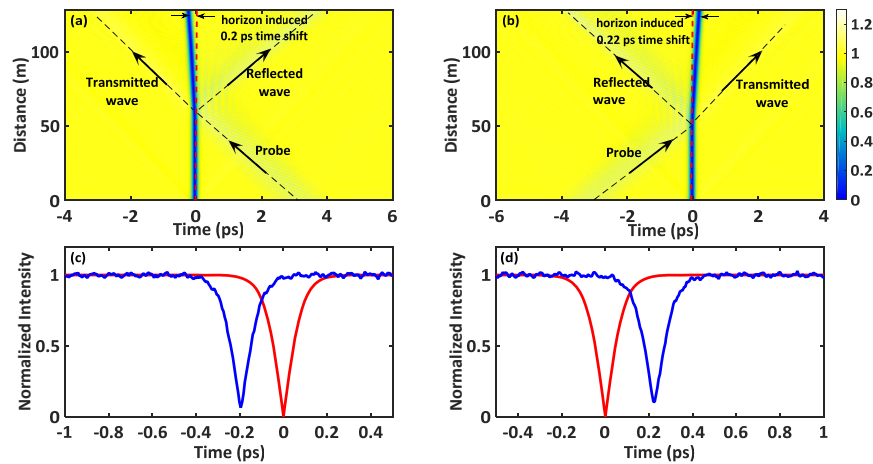

Fig. 3. Numerical results of the manipulated propagation of a dark soliton (186 W) using probe waves with different initial frequencies with a same peak power of 2 W (Left panels: probe wave with frequency located in the green-shaded area; right panels: frequency of probe wave in the yellow-shaded area). Red dotted lines in (a, b) indicate the reference lines for the horizon-induced temporal displacement of the dark soliton. Red and blue curves in (c, d) represent the resulting output dark soliton profiles before and after the collision between the dark soliton and the probe wave, respectively.

Figure 3 summarizes the obtained modeling results based on the NLSE describing the collision between a dark soliton and a weak probe wave with varying carrier frequencies. At the input, the dark soliton is aligned to temporally precede or trail the probe wave to realize the collision process according to their relative frequencies and the resulting different traveling velocities [See Fig. 2(b)]. Figure 3(a) shows that the probe wave is elastically scattered and partially transmitted through an effective refractive index barrier induced by the dark soliton. The dynamical process corresponds to the analogue of white-hole horizon. An important feature here is that the probe wave pushes the dark soliton from its original trajectory, which is attributed to the weak but non-vanishing repulsive force between the soliton and the probe wave benefiting from the typical "anti-particle" character of dark solitons at optical event horizon. The steering of trajectory for the dark soliton takes place in the direction opposite to that of the reflected wave, which is fundamentally contrary to what is the case involving with a bright soliton. It can be seen from Fig. 3(a) that the collision results in an acceleration of the dark soliton with a corresponding 0.20 ps temporal shift at the output relative to its initial soliton center (denoted by red dotted lines). This evolution process has recently been referred as diametrically driven self-acceleration [34]. Based on the energy-speed relation for a dark soliton [22], the increase of the soliton speed is necessarily associated with the energy decay for the soliton. Figure 3(c) shows the intensity profile of the dark soliton before and after the collision, and indicates that the quasi-stationary black soliton

($\phi = 0$) is transformed into an accelerated gray soliton with $\phi > 0$. Thus, it can be shown that the optical event horizon can directly result in the dissipative effect of the dark soliton.

Researchers found that swapping the frequencies of the probe and reflected waves simply changes the dynamics of the optical event horizon [16]. If the original frequency of the probe wave is shifted to the frequency of the reflected wave in case of an analogue of the white-hole horizon, the dark soliton initially trails the probe wave temporally by 3.5 ps for the realization of the interaction between them. Here, the time-reversal symmetry for the black- and white-holes horizons can be invoked: the process that occurs at the black hole horizon is simply the time-reverse of a corresponding process at the white hole horizon. We can see from Fig. 3(b) that the reflection process can cause a deceleration of the dark soliton. The output soliton profile in Fig. 3(d) shows the time delay and dark soliton decay in contrast to its initial temporal profile (denoted by red curve). These observations suggest that the black soliton dissipates energy and is transformed into a decelerated gray soliton with $\phi < 0$. The soliton-probe collision dynamics discussed above demonstrate that we can use the frequency of the probe wave as an effectively controllable variable for all-optical manipulation of dark soliton.
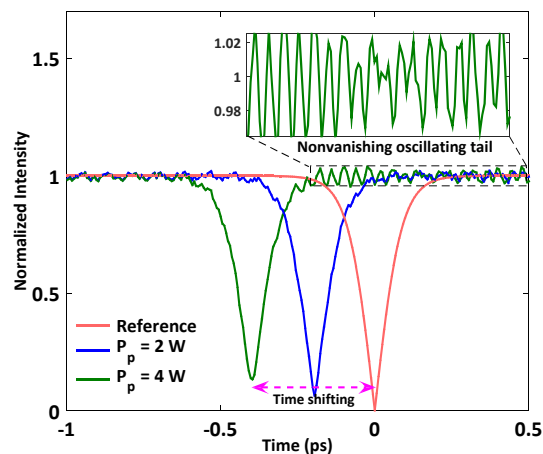

Fig. 4. Output dark pulse profiles for the analogue of white-hole horizon as the peak power of the probe wave is varied, showing that both the soliton decay and the time shift between the dark solitons before and after their interaction with the probe wave can be controlled by adjusting the peak power of the probe wave.

The main idea for a dark soliton manipulation with a weak probe wave at optical event horizon can be characterized by the horizon-induced temporal shift of the dark soliton. We find that both the time shift and the dissipative effect of the black soliton can be investigated by simply adjusting the peak power of the injected probe wave. The obtained output dark pulse profiles in contrast to the injected dark soliton after interaction with the probe wave at two different peak powers of 2 W and 4 W are shown in Fig. 4. A significant increase of the peak power P_p results in a greatly reduced amplitude of the soliton and increasing time delay after the collision: for $P_p = 2$ W (which is the case in Fig. 3) the soliton's amplitude decreases by ~5.9% and the temporal shift of soliton increases to 0.2 ps, while for $P_p = 4$ W the corresponding values are ~14% and 0.39 ps, respectively. Besides, the uniform background is full of a non-vanishing oscillatory tail with similar amplitude, showing that optical event horizon can cause an energy loss for dark solitons in the form of a continuously growing tail, similar to that of a dark soliton confined in boxlike traps [35].

In this section, we have demonstrated that the propagation of dark solitons dressed by the optical event horizon is typically dissipative. In the next section we will develop an analytic description to gain deeper insights.

3.2 Linear-stability analysis of dark solitons at optical event horizon

We now turn our attention to explore an interesting question concerning the existence of stationary dark soliton solution of Eq. (1) and analyze the mechanism behind the dark soliton manipulation with a weak probe wave at group-velocity-led optical event horizon. Given that dark solitons that are similar to the bright one also appear like an effective particle, the linear-stability analysis can be analytically studied based on the adiabatic approximation of the perturbation theory.

Traditionally, the one-dimensional NLSE can be used to analyze the relative strengths of physical effects governing the pulse evolution. We introduce a new term ε to describe the probe wave perturbation. We substitute the following dimensionless variables into Eq. (1) [22]:

$$\tau = T \cdot A_0, \;\; \xi = z / L_D, \;\; U(\xi, \tau) = A(z, T) / A_0, \tag{6}$$

where τ, ξ, U correspond to the normalized time, propagation distance, and pulse envelope with regards to $1 / A_0$, dispersion length $L_D = 1 / (A_0^2 \beta_2)$, and the background amplitude of the dark soliton A_0, respectively. The obtained dimensionless NLSE characterizing the dark soliton evolution $U(\tau, \xi)$ in the normal dispersion regime is shown as following [5, 21]:

$$i \frac{\partial U}{\partial \xi} - \frac{1}{2} \frac{\partial^2 U}{\partial \tau^2} + |U|^2 U = \varepsilon V(\tau) U, \tag{7}$$

where the parameter $\varepsilon = \gamma L_D P_p / A_0^2$ is the strength of the perturbation $V(\tau)$. The perturbation $V(\tau)$, resulting from the reflected portion of the probe wave that is acting upon the dark soliton, can be approximately calculated [7, 36]:

$$V(\tau) \approx R \cdot (D_r' / L_{fiber}) \cdot |A_p(\tau)|^2, \tag{8}$$

where $D_r' = \partial_\omega D(\omega_r)$ is the group velocity mismatch between the dark soliton and the probe wave, and R is the reflection coefficient of the probe wave on the soliton at optical event horizon [7, 33]. The terms on the left-hand side of the Eq. (7) are associated with the fundamental dark soliton [22]. The right-hand side is reserved for perturbation on the dark soliton evolution at optical event horizon. Obviously, the balancing between the two terms in the NLSE (the linear term and the nonlinear term) is altered by the presence of the latter, and then the integrability is broken. In this sense, the wave packets studied here are not true solitons. However, without loss of generality we still use this term to refer to the non-dispersing pulses formed by nonlinearity.

To analyze the linear stability of this dark soliton pulse, we find solutions of Eq. (7) in the following form:

$$U(\xi, \tau) = e^{-i\xi} [\nu_s(\tau) + \delta(b(\tau) e^{-i\kappa\xi} + \overline{c}(\tau) e^{i\overline{\kappa}\xi})], \tag{9}$$

where $b(\tau), c(\tau)$ are normal-mode perturbations, $\kappa = \kappa_r + i\kappa_i$ is the eigen-frequencies of this (generally complex) normal mode, and $\delta \ll 1$. Importantly, the appearance of a complex eigen-frequency always results in a dynamic instability while a linearly stable configuration is equivalent to $\kappa_i = 0$ (i.e., all eigen-frequencies are real). Substituting this perturbed solution into Eq. (7) and linearizing with respect to δ, we obtain the following linear-stability eigen-frequency problem:

$$\mathbf{L}\boldsymbol{\psi} = \kappa\boldsymbol{\psi}, \tag{10}$$

where

$$\mathbf{L} = \begin{pmatrix} -\dfrac{1}{2}\partial_\tau^2 + \varepsilon V(\tau) - 1 + 2v_s^2 & v_s^2 \\ -v_s^2 & \dfrac{1}{2}\partial_\tau^2 - \varepsilon V(\tau) + 1 - 2v_s^2 \end{pmatrix}, \quad \psi = \begin{pmatrix} b \\ c \end{pmatrix} \qquad (11)$$

This eigen-frequency problem is then solved numerically using the Fourier collocation method [37]. Example of the whole stability spectrum for the stationary dark soliton under the perturbation of a probe wave with $\varepsilon = 7 \times 10^{-4}$ (corresponding to $P_b \approx 4$ W) is shown in Fig. 5(a). It can be observed that the dark solitons are unstable in an apparently dynamic manner as a result of the eigen-frequencies with nonzero imaginary part in the spectrum.
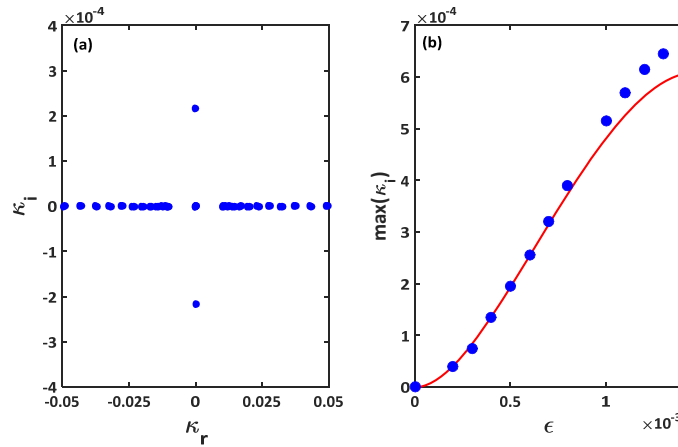

Fig. 5. (a) Corresponding spectral plane (κ_r, κ_i) of the eigenvalues. It shows a pair of imaginary eigenvalues demonstrating the dynamical instability of the dark soliton solution. (b) the imaginary part of the eigenvalue κ_i as a function of ε. Solid red curve represents the analytical prediction while blue circles correspond to the numerical results.

In order to well understand these instabilities and obtain an analytical estimate for the relevant eigen-frequencies, we introduce the Newton's particle result in [38]. One can show in a straightforward manner that the function

$$M'(s) = \int_{-\infty}^{+\infty} \frac{\partial V}{\partial \tau} \left[1 - \tan h^2 (\tau - s) \right] \mathbf{d}\tau \qquad (12)$$

should vanish in order to survive the dark soliton with the perturbation $V(\tau)$, which means the equation $M'(s) = 0$ has at least one root s_0 [38]. Then, the stability of the dark soliton solution presented above is dependent on the sign of the second derivative of $M(s)$. Generally, an instability will be occurring with one imaginary eigenvalue pair for $\varepsilon M''(s_0) < 0$, and with exactly one complex eigenvalue quartet for $\varepsilon M''(s_0) > 0$ [38]. The instability is dominated by the eigen-frequency of Eq. (10), which bifurcates from the origin as long as the perturbation is present, in sharp contrast to the situation for the higher-order bright counterparts where an instability occurs only when the magnitude of perturbation exceeds a minimum threshold [21]. We find that the relevant eigen-frequencies are determined by the following quadratic characteristic equation [38],

$$\lambda^2 + \frac{\varepsilon}{4} M''(s_0)\left(1 - \frac{\lambda}{2}\right) = O(\varepsilon^2), \tag{13}$$

where the perturbation is given by Eq. (7), and eigenvalues λ, which are related to eigen-frequencies κ through $\lambda^2 = -\kappa^2$. Assuming that s_0 satisfies the equation $M'(s) = 0$, we can evaluate $M''(s_0)$ explicitly to obtain:

$$M''(s_0) = 2\int_{-\infty}^{+\infty} \frac{\partial V}{\partial \tau} \tan h(\tau - s_0)\operatorname{sech}^2(\tau - s_0)\mathbf{d}\tau \tag{14}$$

To this end, combining the result of Eq. (13) and Eq. (14) yields an analytical prediction for the magnitudes of relevant eigenvalue.

Figure 5(b) shows the pertinent analytical solution (depicted by red solid curves) in contrast to the corresponding numerical results (depicted by blue points). For smaller perturbation parameter ε, the numerical results are in excellent agreement with the analytical one. The distinct deviation for larger perturbation values is attributed to the assumption that the soliton remains unaffected during its interaction with the probe wave that is not the case even for a weak probe wave. The exponential growth rate of the instability is determined by the magnitude of eigen-frequencies imaginary part, and then the dark soliton at optical event horizon becomes mobilized and weakened through the generation of a continuously growing tail from the right of the primary soliton. The larger the imaginary part of eigen-frequencies is, the more the energy of dark soliton is lost. These results suggest that the fundamental features of the dark soliton propagation can be manipulated by careful power adjustment of the probe wave at optical event horizon. As the perturbation ε is increasing up to a certain value, the probe wave at optical event horizon may precipitate the "catastrophic collapse" of the dark soliton. As shown in [15], the interaction between a dark soliton and an intense probe wave causes the disintegration of the dark soliton.

3.3 Dark solitons collision induced by dual-probe waves at optical event horizon

Based on the time-reversal symmetry character for the evolution dynamics presented above, it should be interesting to explore what will happen when the white-hole and black-hole event horizons are combined together. In this situation we consider the input optical fields that are consisted of a pair of well-separated dark solitons and two probe waves located outside of them as following:

$$A(0, T) = \sqrt{P_p}\left\{\exp\left[-\left(\frac{T + t_1}{T_1}\right)^2\right]\exp(i\Delta\omega_1 T) + \exp\left[-\left(\frac{T - t_1}{T_1}\right)^2\right]\exp(i\Delta\omega_2 T)\right\} + A_{ds2}(T) \tag{15}$$
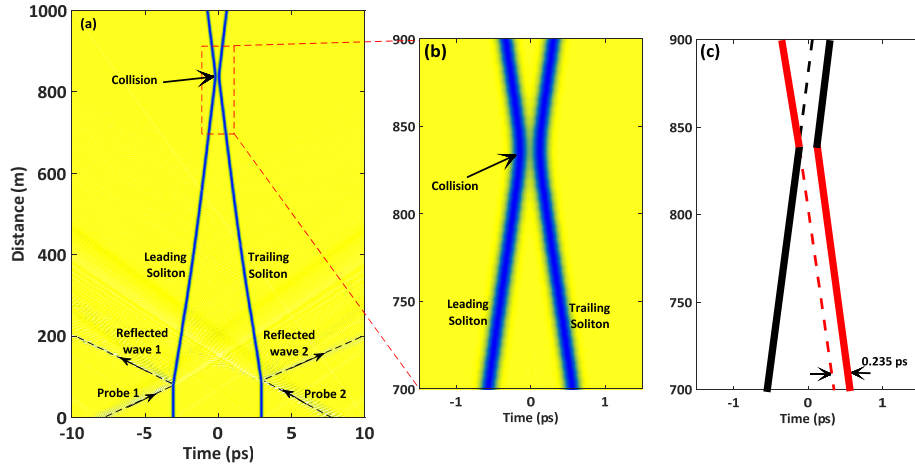
Fig. 6. (a) Density maps of the temporal evolution of interaction between two dark solitons and dual-probe waves in an optical fiber. The collision between both dark solitons will occur due to an acceleration or deceleration of them induced by the probe wave at optical event horizon; (b) magnified collision region; (c) illustration on how the dark solitons pass through each other, involving undergoing a time shift but maintaining their direction (different colours are used to define each soliton).

The pair of dark solitons is

$$A_{ds2}(T) = -u_0 \tan h[u_0(T + t_2)], \tag{16}$$

where $-\infty < T < 0$, and

$$A_{ds2}(T) = u_0 \tan h[u_0(T - t_2)], \tag{17}$$

where $0 < T < +\infty$. Here, t_1 and t_2 represent the launch position of the probe wave and the soliton pulse, respectively, whereas $\Delta\omega_1$ and $\Delta\omega_2$ are the relative frequency of both probe waves. It should be noted that the position of both probe wave frequencies must be symmetrical to the group-velocity matched point in Fig. 2 to ensure the time reversal quality for the corresponding evolution process. In this case, we will be able to observe the occurrence of soliton-soliton collision and the tunneling behaviour between two dark solitons. It can be seen from Fig. 6(a) that both dark solitons pass through one another in the course of collision, and then continue to propagate with an unchanged velocity. As can be seen from the intensity evolution in Fig. 6(b) alone, the interaction between both dark solitons seem to be repulsive. However, they are in fact transmitted, acting as a discontinuous jump in position relative to the original trajectory as a result of the collision [See Fig. 6(c)]. The apparent node between both dark solitons, resulting from the interference of the two wave packets, leads to a negligible intensity dip at the center of the collision [39, 40]. The jump is a consequence of the nonlinearity interaction of the system. Since the temporal shift of solitons is significantly dependent on the grayness of the colliding solitons [41], the collision-induced time shift of solitons can also be manipulated by adjusting the strength of the incident probe waves at optical event horizon.

To fully understand the dynamics of dark soliton-soliton collision under the action of the probe wave, the position where both dark solitons eventually collide and the time shifting for both solitons as a function of the initial peak power of the incident probe wave are calculated and shown in Fig. 7. The initial temporal width of the incident probe waves is fixed to 800 fs. It is clear that the distance at which the collision of both dark solitons occurs decreases significantly with the increasing peak power of incident probe waves. This is attributed to the

significant variation of the traveling speed and grayness of the dark solitons induced by the increasing peak power of the probe waves at optical event horizon. Meanwhile, the collision-induced time shifting for both solitons is decreased when the peak power of probe wave is increased, as can be seen from the blue filled circle lines in Fig. 7. We can conclude that adjusting the peak power of the incident probe waves at optical event horizon is one of most effective and suitable means to control the collisional dynamics of dark solitons.
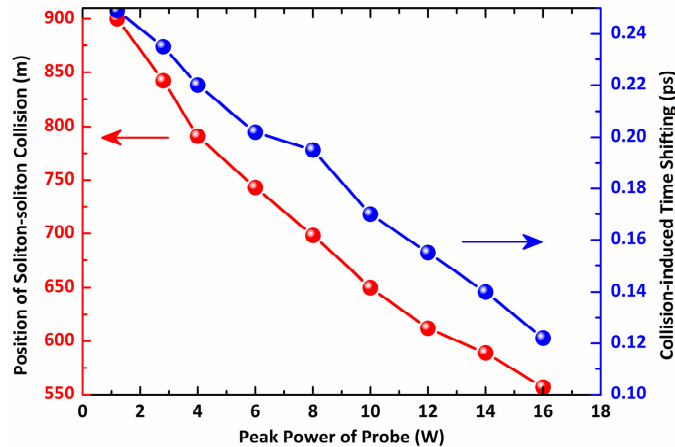

Fig. 7. Position of dark soliton-soliton collision and the collision-induced time shifting for both solitons as a function of the peak power of the probe wave. The red-filled circle lines correspond to the collision position of both dark solitons while the temporal shift of solitons induced by twin-soliton collision is shown by the blue-filled circle lines.

4. Conclusions

In conclusion, we have shown that the analogy between event horizons and the nonlinear reflection of a weak probe wave onto a dark soliton opens innovative perspectives in the control of light. The optical event horizon is demonstrated to have a typical dissipative effect on dark solitons where the black soliton is decayed into a 'new' gray soliton (with lower energy) with non-vanishing oscillating tail, in sharp contrast to the situation where the bright soliton interacts with the dispersive wave. The soliton grayness can be effectively controlled by adjusting the peak power of the probe wave with the optical event horizon, corresponding to the manipulation of the dark soliton's speed. However, whether the gray soliton is accelerated or decelerated is significantly dependent on the region where the selected frequency of probe wave is located. To explore the nonlinear mechanism behind the dark soliton manipulation with the probe wave, we develop a linear-stability eigenvalue problem by the perturbation theory which provides some insights for the dark soliton statics and dynamics, especially the catastrophic collapse. In the soliton-soliton collision dynamics induced by the probe waves, both dark solitons pass through one another and emerge from the collision unchanged in velocity, with a mutual temporal shift. The position at which both dark solitons eventually collide and the collision-induced time shift of both solitons can be effectively controlled by adjusting the intensity of the probe waves. These results can be proposed as a candidate to realize the photonic transistor-like action and provide further insights into the collisional dynamics of dark solitons in a more controllable manner.

Funding